JMEPEG (2016) 25:831–838
DOI: 10.1007/s11665-016-1915-9

1059-9495/$19.00

Influence of Dispersion in Composites of Chopped PAN-Based Carbon Fiber Modified by Dodecyl Ether Carboxylate

B. Wu, G. Zheng, Y.J. Liu, Y. Sun, and L. Wang

(Submitted July 4, 2015; in revised form November 22, 2015; published online January 29, 2016)

In this article, dodecyl ether carboxylate (AECNa) was prepared by dodecanol polyoxyethylene, sodium chloroacetate, and sodium hydroxide and employed as a treatment agent for PAN-based carbon fiber (CF) surface. The results show that the optimum adsorption amount of AECNa modifying CF was determined to be 4.0 mg/g. In addition, the equivalent variation regularity is obtained the CF surface charge properties and its dispersion behavior. The optimal dispersion effect of the short CFs in epoxy matrix is achieved when the surface charges reach the maximum by quantitative measurement using Faraday cup; the surface morphology and wettability are improved depending on the field emission scanning electron microscopy, Thermogravimetry, x-ray photoelectron spectroscopy, and monofilament contact angle testing. Furthermore, the flexural strength and modulus of the treated CF composite were proven to advance by flexural tests.

Keywords charge, composite, dispersion, dodecyl ether carboxylate, PAN-based carbon fiber, surface

1. Introduction

Polyacrylonitrile (PAN)-based carbon fibers (CFs) are formed when polyacrylonitrile is subjected to three stages of reaction, re-oxidization, oxidation, and carbonization, which forms fibers with a carbon content of more than 90%. In recent years, CFs have been widely employed in the aerospace, energy, and marine industries, because of their outstanding properties including, high specific strength and stiffness, low density, and heat resistance, which made them useful in composite technology, including the use of the chopped CFs as fillers in polymer matrices, which has attracted particular interest due to their facile preparation and low cost (Ref 1, 2).

During the process of preparing chopped CF-reinforced composites, the strength and modulus of the composites are influenced by the dispersion and adhesion of fibers in the matrix. Strong Van der Waals forces and low surface free energy result from surface irregularities and the small amount of chemically active groups on the CF surface, which leads to undesirable agglomeration of the chopped CF in a composite (Ref 3, 4). Moreover, to further improve CF dispersion in the matrix, the surface activity of the CF can be enhanced by modifying agents; the optimum conditions of this surface treatment are an important factor that can affect ultimate mechanical properties of resulting composites. In a previous work, Wang et al. (Ref 5, 6) studied the aqueous dispersion of short CF treated with hydroxyethyl cellulose and other agents. Park (Ref 7) described the dispersion of short plasma-treated CF in a phenolic resin. The optimum treatment conditions of the dispersant were determined using SEM or by direct observation (Ref 5-9), which was a small portion in the investigation of the CF surface morphology. In conventional research concerning the dispersion of CFs, measurement of CF surface charge as a factor in identifying optimum dispersants for modifying CF has not been extensively investigated with regard to CF dispersion.

In this study, CFs were treated with dodecyl ether carboxylate (AECNa) which was formed by carboxymethylation of dodecanol polyoxyethylene (AEO), sodium chloroacetate, and sodium hydroxide (NaOH). In general, the resulting AECNa containing a carboxylic acid ester as the hydrophilic group and a long-chain fatty alcohol as the lipophilic group had a high molecular weight with long polymer chains. When AECNa was added, electrostatic and adhering interactions are responsible for the adsorption of molecules (Ref 10, 11). In addition, the surface charges of treated CFs were quantitatively determined using a Faraday cup. The surface morphology, chemical groups, and wettability of the treated and untreated CFs were ascertained using a field emission scanning electron microscopy (FE-SEM), thermogravimetry (TGA), x-ray photoelectron spectroscopy (XPS), and monofilament contact angle testing. Moreover, the flexural properties of the fabricated composites were also determined.

2. Experimental

2.1 Materials

The PAN-based CF (T300-6K) with a diameter of about 7 μm, linear density of 204.5 g/km and a volume density of

B. Wu and **G. Zheng**, School of Material Science and Engineering, Tianjin Polytechnic University, Tianjin 300387, China; and Tianjin Engineering Research Center of Textile Fiber Interface Treatment Technology, Tianjin 300270, China; **Y.J. Liu** and **Y. Sun**, Tianjin Engineering Research Center of Textile Fiber Interface Treatment Technology, Tianjin 300270, China; and School of Environment and Chemical Engineering, Tianjin Polytechnic University, Tianjin 300387, China; and **L. Wang**, School of Material Science and Engineering, Tianjin Polytechnic University, Tianjin 300387, China. Contact e-mail: zhengguo0703@126.com.

1.772 g/cm^3 was purchased from Jilin Chemical Fiber Co., Ltd (Jilin, China). The epoxy resin used in this study was composed of part A, which was epoxy 618 (bisphenol A epoxy), and part B, a curing agent 2-ethyl-4-methylimidazole purchased from the Nantong Stars Synthetic Material Co., Ltd. Acetone (purity ≥ 99%) was obtained from Tianjin Wind Ship Chemical Technology Co., Ltd. (Tianjin, China). AEO was obtained from the Tianjin Polytechnic University for Textile Auxiliary Co., Ltd. (Tianjin, China). Sodium chloroacetate (purity ≥ 99%) was supplied by the Tianjin Guangfu Fine Chemical Research Institute. All of the other chemicals including H_2SO_4 and NaOH were of analytical grade and purchased from Tianjin Kermel Chemical Reagent Co., Ltd. (Tianjin, China). Distilled water was used during the synthesis and dispersion processes.

2.2 Synthesis of AECNa

The AECNa synthesis procedure can be described as follows. In a typical reaction, AEO and NaOH were poured into a four-neck flask (500 mL) equipped with a thermometer, reflux condenser, vacuum pump, and a mechanical stirrer, with a stirring speed of 300 r/min. The mixture was reacted for 3 h at a temperature of 160 °C under a nitrogen atmosphere and 0.09 MPa vacuum. Then, sodium chloroacetate was added to the flask to react with the product of the first step and the subsequent reaction mixture was incubated at 90 °C for 4 h. At the end of this time, a large amount of white precipitate formed. 100 mL of ethanol was added to the precipitate to dissolve the AECNa. The mixture was then separated by centrifuging to remove unwanted products and distilled at 80 °C for 30 min to obtain the final crude yellow AECNa mucilage. The mucilage was finally dried in an oven at 60 °C for 2 h to yield the final product (Ref 12, 13). The principles of synthesis method of AECNa are shown in Scheme 1.

2.3 Surface Treatment and Dispersion of CF

The commercial PAN-based CFs were initially extracted by Soxhlet extractor using water and acetone (1:4 in volume) for 2 h to remove the surface organic impurities. The pretreated CFs were then dried in an oven for 2 h at 85 °C and weighed. Then, the pretreated CFs were submerged in the AECNa emulsion for 30 min with a weight ratio of CFs to emulsion of 1:100. The treated CFs were then dried in a vacuum oven at 100 °C (Ref 14).

The treated chopped CFs (0.01 ± 0.001 g) with a length of 10 mm were placed in a clean 100-mL beaker containing 10 g of epoxy resin and incubated at 90 °C, to ensure the dispersion of the CFs in the resin. This mixture of CFs and epoxy resin was stirred using a glass rod and allowed to stand for 10 mins. The dispersion of the treated CFs was evaluated by direct observation (Ref 5, 7).

2.4 Preparation of Chopped CF/Epoxy Resin Composites

The surface-treated, chopped CFs and epoxy resin were added to a mold with 4 mm thickness and heated at 90 °C. The curing agent with a weight ratio of epoxy:curing agent of 1:5 was added and evenly stirred into the mixture. The CF/epoxy resin composite was prepared by stacking two plies of plate and pressing with a hot press, isothermally at 90 °C for 2 h, according to the manufacturer instructions. The photos of the composite samples are shown in Fig. 1. In order to determine flexural property of the composite, it was cut to the dimensions of 80 × 10 mm^2 with 4 mm thickness (Ref 15, 16).

2.5 Surface Charge Determination

The surface charge of the CF was determined using a Faraday cup (ZF-611, China) at 20 °C and 40% RH. An electrometer was used to measure the surface charge by detecting the voltage accumulation across a capacitor of a known capacitance. The charge-to-mass ratio (C/g) was measured. The capacitor consists of two parallel metal cups separated at a set distance by insulation (shown in Fig. 2). Approximately 0.5 g of CFs were glued to the inner cylinder, and a voltage difference resulted between the two cups. The measurements were repeated ten times, and the average value was calculated (Ref 17-19).

2.6 Characterization

The surface properties of the AECNa emulsion including surface tension and contact angle were measured using an automatic surface tensiometer according to the BSI standard BSEN14370-2004 and by optical contact angle measurement. The CF monofilament contact angle measurement with water was performed using a precision contact angle measuring instrument (Kruss DSA100M, Germany). Three-point bending tests were conducted on composite samples using an Instron 3369, carried out with a cross-head speed of 2 mm/min for the bar-shaped samples of 80 × 10 mm^2 with 4 mm thickness according to ASTMD790.

The chemical structures of the AECNa sample were characterized by FTIR (Bruker TENSOR37, Germany), obtained from KBr pellets over the range of 500 to 4000 cm^{-1} on the spectrophotometer. The surface morphologies of the treated and untreated CFs were observed employing FE-SEM (HITACHI S-4800, Japan), with samples fastened on a metal holder by twin adhesives and sputter-coated with thin gold coating prior to SEM testing. TGA of all samples was carried out using a thermal analyzer (NETZSCH STA409PC, Germany) under a dynamic atmosphere of nitrogen at the heating rate of 10 °C/min from 50 to 600 °C with a sample mass of 10.0 mg. High-energy-resolution XPS (ThemoFisher

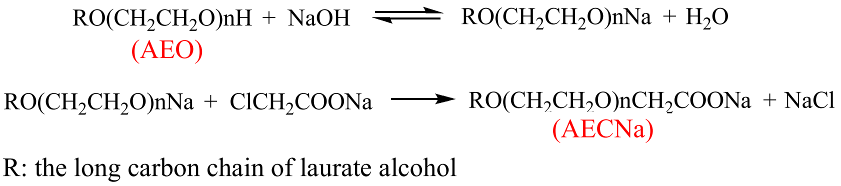

$$\underset{\text{(AEO)}}{RO(CH_2CH_2O)nH} + NaOH \rightleftharpoons RO(CH_2CH_2O)nNa + H_2O$$

$$RO(CH_2CH_2O)nNa + ClCH_2COONa \longrightarrow \underset{\text{(AECNa)}}{RO(CH_2CH_2O)nCH_2COONa} + NaCl$$

R: the long carbon chain of laurate alcohol

Scheme 1 Principles of synthesis method of AECNa

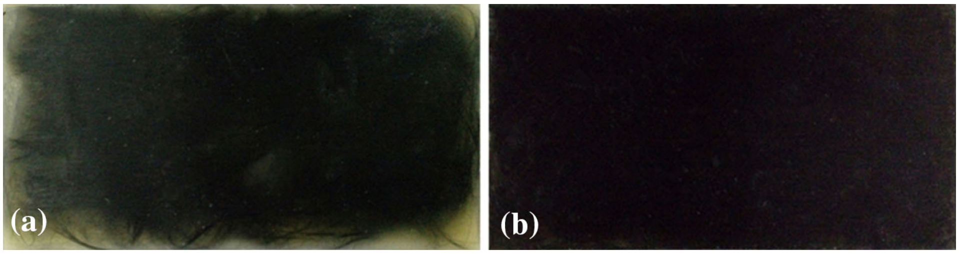

Fig. 1 Photos of the composite samples: (a) CF composite and (b) AECNa-CF composite

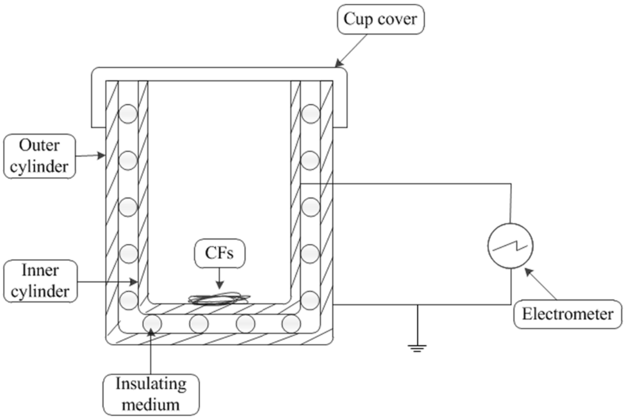

Fig. 2 Schematic of Faraday cup to determine surface charge of CFs

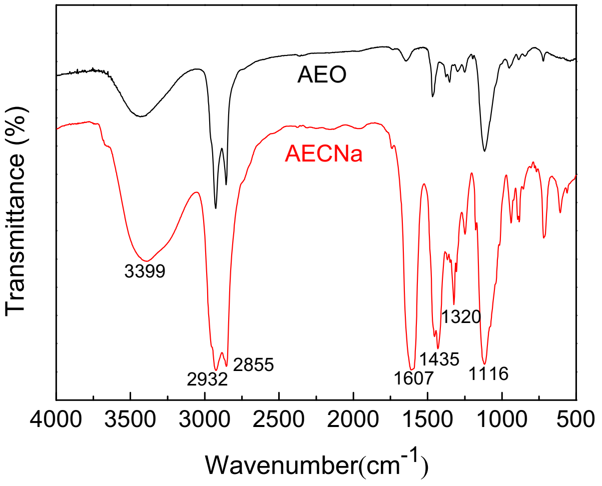

Fig. 3 FTIR (KBr) spectra of the AEO and AECNa

K-Aepna, USA) was performed using monochromatic x-rays to analyze the surface chemical composition of select samples.

3. Results and Discussion

3.1 FTIR of the AECNa

The significant chemical changes of the synthesized products were confirmed by the samples' FTIR spectra. Figure 3 shows the differential spectrum, which was obtained from the AEO and AECNa. The strong bands at 2855, 1435, and 1320 cm^{-1} in AECNa spectrum correspond to the bending vibration for the asymmetric stretching vibration of C-H, bending vibration of CH_2, and bending vibration of CH_3. The absorption band at 1116 cm^{-1} for the C-O-C stretching was due to polyoxyethylene ether groups, which structure both in AEO and AECNa. But the band at 1607 cm^{-1} for the O=C-O stretching of carboxylic acid group was obviously enhanced due to the different structures of AECNa compared to AEO. Moreover, the reason for the occurrence of the weak band in the spectrum of AEO is that the reagent (AEO) is of industrial grade, which has little impurity. These characteristic peaks confirm that AECNa resulted from the synthesis reaction. The peak at 3399 cm^{-1} is for C-OH which can be attributed to the residual raw material in the reaction mixture.

3.2 Analysis of AECNa Emulsion on the Dispersion of CF

The results of surface tension measurements of the AECNa emulsion and emulsion contact angle of CF with different concentrations are presented in Fig. 4(a) and (b). Critical Micelle Concentration (CMC) is an important characteristic of surfactant, including AECNa. At this point, the surfactant molecules distribute ultimately orderly on the surface of emulsion, and the surface tension of surfactant emulsion reaches the minimum. The emulsion surface tension and contact angle reached the minimum values of 29.75 mN/m and 43.69° at the concentration 0.5 wt.% AECNa, respectively. It can be concluded from that the CMC of AECNa is 0.5 wt.% and the best spreadability of the emulsion on the CF surface was achieved at this concentration. Moreover, the contact angle reaches a minimum value when the concentration of AECNa is up to 0.5 wt.% and then it increases with concentration of AECNa being greater than 0.5 wt.%, which is due to the surface energy of the interface of AECNa emulsion and CF reaching a maximum value.

The impact of the amount of AECNa adsorption on the dispersion of CF was investigated, and the results are shown in Fig. 5. The untreated CFs tended to agglomerate in the epoxy resin, which was attributed to the high van der Waals forces between the monofilaments due to their small diameter, surface flaws, and low surface activity. However, the dispersibility of the CFs that were treated using AECNa was much higher and the chopped CFs were completely dispersed in the resin matrix at a loading of 4.0 mg/g. This trend may result because the interfacial tension of treated CFs and matrix is less than that of untreated fibers resulting from the affinity of the AECNa on the interface of the treated fibers and the epoxy resin. Furthermore, the lipophilic groups in AECNa are adsorbed in an orderly manner on the CF hydrophobic surface at low concentration,

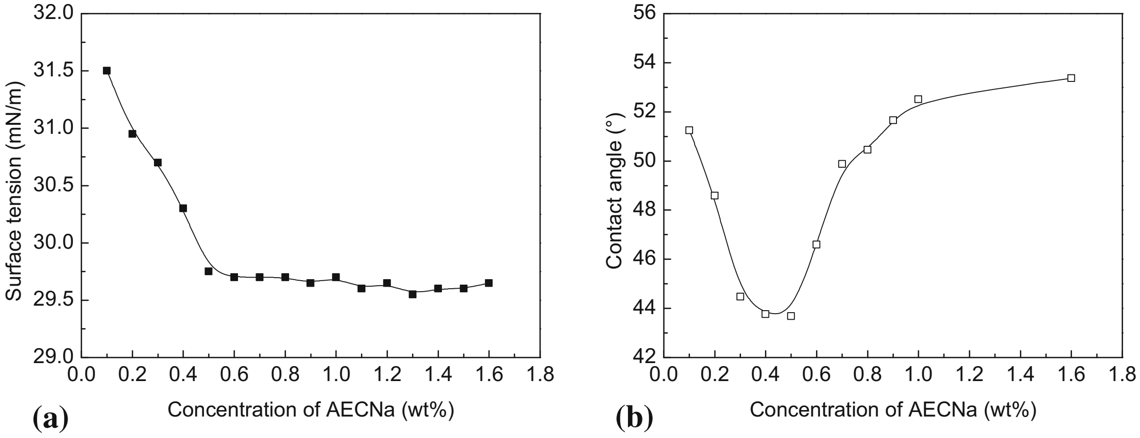

Fig. 4 Influence of concentration of AECNa on the emulsion surface properties

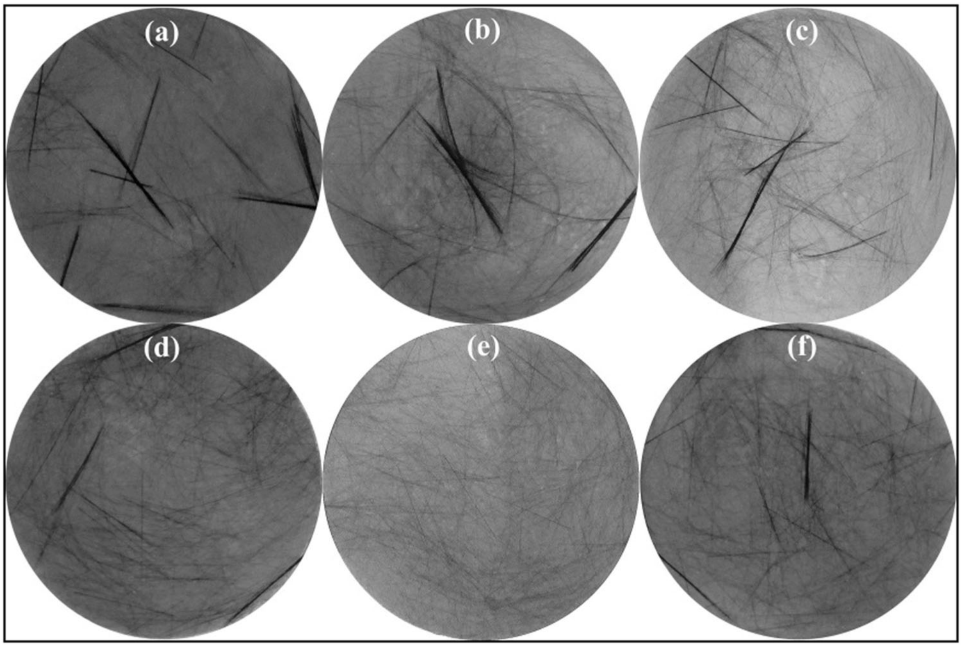

Fig. 5 Photos of dispersion effect of the CFs treated by AECNa with different adsorption amounts: (a) untreated, (b) 1.0 mg/g, (c) 2.0 mg/g, (d) 3.0 mg/g, (e) 4.0 mg/g, and (f) 5.0 mg/g)

and the hydrophilic groups allow the surface of CFs to form a uniform charge layer (Ref 20, 21). As illustrated in Fig. 6, the surface charge of the untreated CF is 0.025 μC/g which is positive. Nonetheless, surface charge is gradually converted to a negative value as the adsorption of AECNa increases. When the amount of adsorbed AECNa reached 4.0 mg/g, the surface charge attained its maximum value of −0.126 μC/g. The dispersibility of CFs was enhanced as the repulsive forces between CF monofilaments increased (Ref 22, 23). However, these charges decreased initially as the amount of adsorbed AECNa increased, and then remained constant, because of the supersaturated adsorption of the electroneutral micelle, which produced an association between hydrophilic groups on the CF surface. Hence, the adhesive force is greater than the repulsive force between the monofilaments, leading to a decrease in the CF dispersibility (Ref 22, 24).

3.3 Surface Properties of Untreated and Treated CF

The FE-SEM images of the untreated and AECNa-treated CFs are shown in Fig. 7. It was found that a heterogeneous agent layer was formed on the fiber surface after treatment with AECNa at an adsorption amount of 4.0 mg/g. The coarse surface of the untreated CF was found to be smooth. The cohesive force between two monofilaments treated with an adsorption amount of 4.0 mg/g is lower than the untreated CF, resulting in satisfactory dispersion of the CFs in the epoxy resin. However, a pileup of pellets of the treatment agent was observed in the sample when the adsorption amount of the agent was 5.0 mg/g (Fig. 6f).

TGA curves are shown in Fig. 8. As can be seen from Fig. 8(a), the AECNa starts to lose weight at about 100 °C and completes at about 400 °C. As can be seen from Fig. 8(b) and (c), from 100 to 400 °C, the mass attenuation rate of AECNa-

CF is about 0.4% more than the attenuation rate of CF, which confirms that the amount of AECNa present on the CF is 4.0 mg/g and the distribution of AECNa on the CF surface is uniform, so the dispersibility of AECNa-CFs is improved.

Examination of the wide XPS spectra of CF and AECNa-CF (Fig. 9) shows that the chemical elements present on the surface of the CF were mainly carbon, oxygen, and nitrogen. In general, the content of O in the AECNa-CF was 28.3% higher than that in the untreated CF, while the content of C appeared to be 12.1% lower. When compared to the untreated CF, the content of Na in the AECNa-CF surface obviously increased.

The C1s XPS spectra of the CF and AECNa-CF are shown in Fig. 10(a) and (b). The spectra can be resolved into four different component peaks including graphitic carbon (C-C, 284.5 eV), carbon-bonded alcohol or ether groups (C-OH or C-O-C, 285.6 eV), carbonyl groups (C=O, 286.6 eV), and carboxyl or ester groups (COOH or COOR, 288.3 eV) by the XPS-peak-differentiating analysis (Ref 25-27). Compared to the CF before treatment, the peak at 284.5 eV weakens, while the peaks at 285.6 and 288.3 eV increase significantly. Therefore, the XPS spectra suggest that the AECNa is uniformly distributed on the carbon fiber surface.

Photographs of a water drop on the untreated and treated CF monofilaments are shown in Fig. 11(a) and (b). It can be concluded from these photos that the contact angle of water on the AECNa-treated CF monofilament is 74.5°, which is 35.8% less than that of untreated fiber (116.1°). These results suggest that AECNa molecule is adsorbed on the surface of treated CF, which can improve the surface free energy and wettability of the fiber by increasing the number of hydrophilic functional groups on the fiber surface (Ref 28, 29).

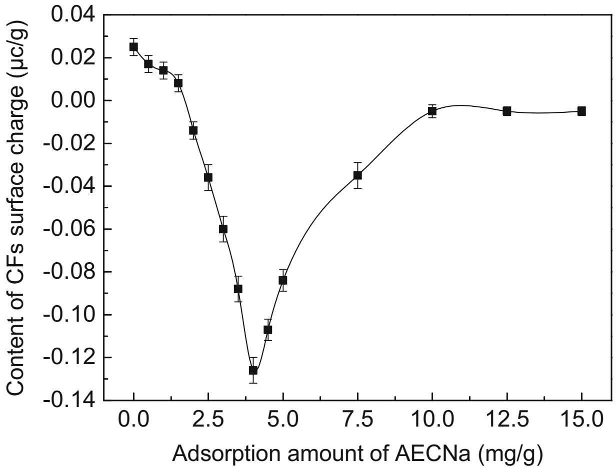

Fig. 6 Change of the surface charge of CFs treated by AECNa

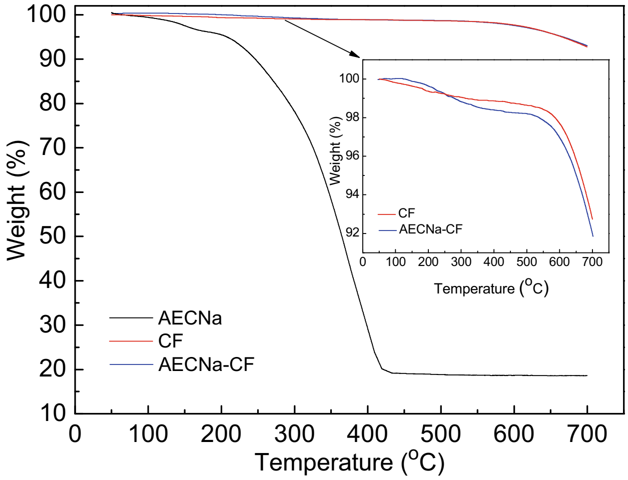

Fig. 8 TGA curves of treatment agent and CF samples: (a) AEC-Na, (b) CF, and (c) AECNa-CF

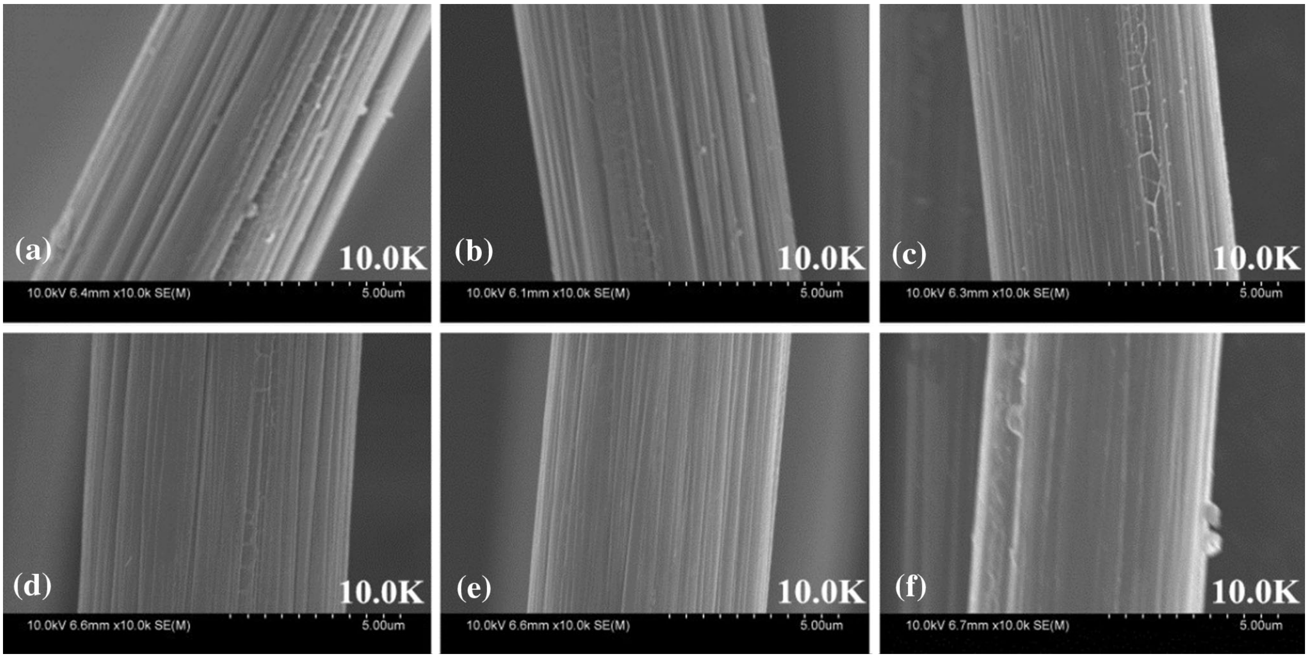

Fig. 7 FE-SEM images of CFs treated by AECNa: (a) untreated, (b) 1.0 mg/g, (c) 2.0 mg/g, (d) 3.0 mg/g, (e) 4.0 mg/g, and (f) 5.0 mg/g)

3.4 Flexural Property of the Chopped CF/Epoxy Resin Composite

Experimental data from flexural tests for all specimens are shown in Table 1. These results suggest that with a fixed CF content (1.0 wt.%), the flexural strength and modulus of composites prepared using AECNa-treated CFs were higher than those of composites prepared using untreated CFs. Additionally, with an AECNa adsorption amount of 4.0 mg/g, the treated chopped CF/epoxy resin composites were found to have the flexural strength of 2.5 times that of the untreated one.

Figure 12 shows the SEM images of the fractured surface of the composites. The CFs are randomly dispersed in the matrix resin. There are some holes in the composite formed by pulling CFs out of the matrix resin during the mechanical test as shown in Fig. 12(a). It means that the adhesion of the CF and the epoxy resin is very poor. However, it is easy to find fewer holes in the AECNa-CF/epoxy resin composite but to find some attached matrix resins on the surfaces of the CFs in Fig. 12(b). Thus, it reveals that the interfacial adhesion of CF and epoxy resin is improved by treating CFs with AECNa. This improve-

Table 1 Flexural properties of chopped CF/epoxy resin composite samples

Adsorption amount of AECNa (mg/g)	Average flexural strength (MPa)	Average flexural modulus (GPa)
0	91 ± 5	2.85 ± 0.25
1.0	102 ± 3	2.90 ± 0.10
2.0	135 ± 4	3.37 ± 0.13
3.0	196 ± 3	4.20 ± 0.12
4.0	228 ± 3	4.46 ± 0.12
5.0	175 ± 5	4.01 ± 0.18

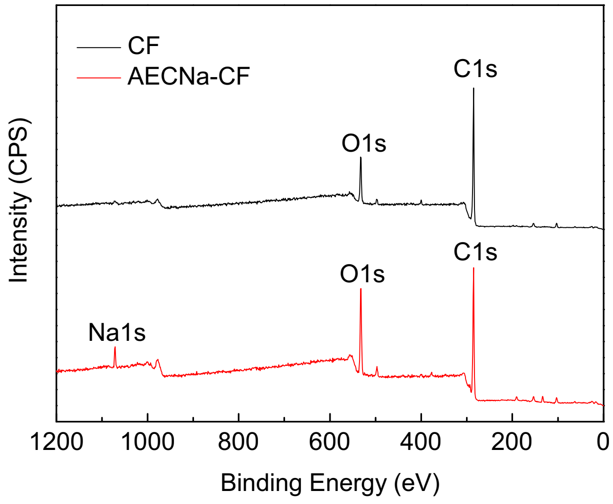

Fig. 9 XPS spectra of CF and AECNa-CF

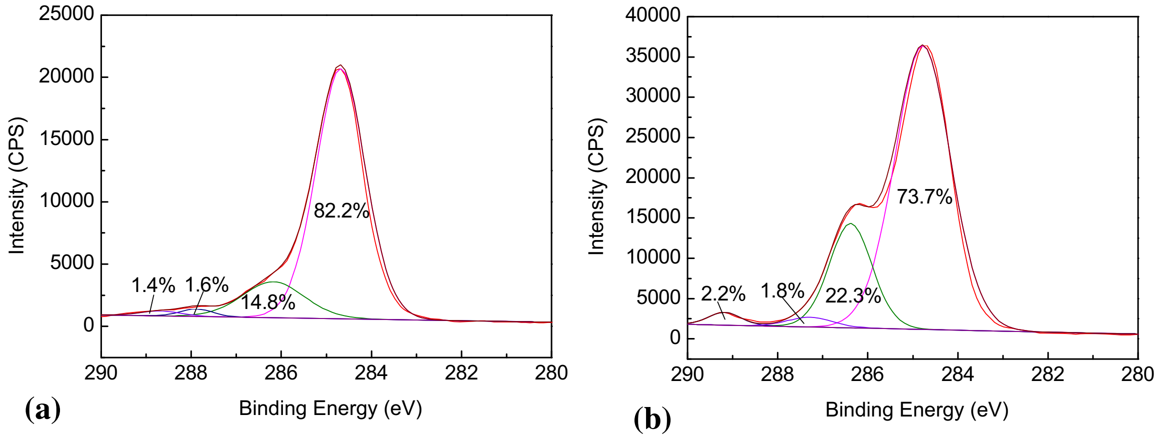

Fig. 10 C1s XPS spectra of CF and AECNa-CF: (a) CF and (b) AECNa-CF

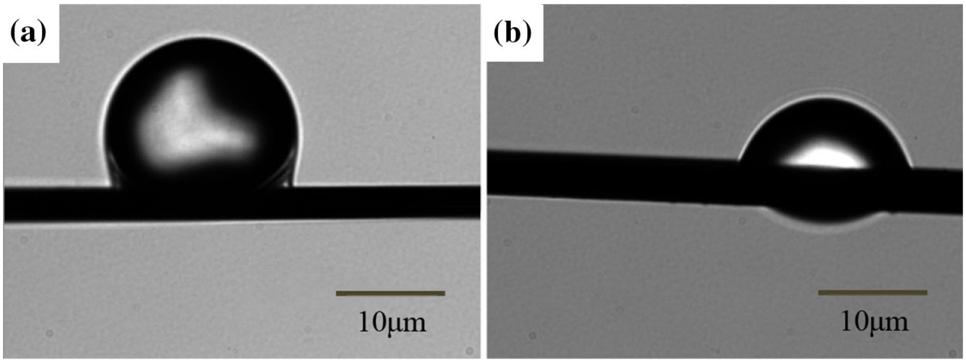

Fig. 11 Photographs of a water drop on untreated and treated carbon fiber monofilaments: (a) CF and (b) AECNa-CF

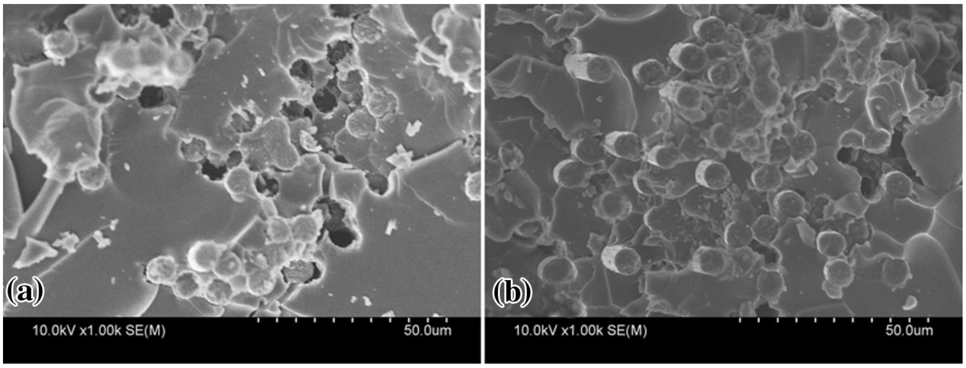

Fig. 12 FE-SEM images of the fractured surfaces of the CF/epoxy resin composites: (a) CF composite and (b) AECNa-CF composite

ment is attributed to the higher dispersibility of the treated CFs in the epoxy resin. In addition, when an external force is applied to the composite, the interfacial shear stress along the fiber axial load is relatively uniform because of the complete dispersion of treated chopped CF in the matrix (Ref 30, 31). By contrast, there were stress defects in the untreated CF composite, which resulted from the poor dispersion of these untreated CFs, leading to a decrease in the interfacial adhesion between the fibers and the matrix. This was a direct result of the decrease in the relative length-to-diameter ratio in the area of monofilaments reunion (Ref 32).

4. Conclusions

AECNa was prepared and successfully employed as a novel treatment agent for CF surface modification. The experimental data confirmed the optimum adsorption amount of AECNa in the pretreatment solution to be 4.0 mg/g. It was believed that this optimum amount could improve the surface blemishes on the fibers and the free energy of CFs. The characterization results for the CF surface proprieties suggested that there was a direct relationship between the dispersivity of the CFs and the resulting CF surface charge properties. The optimum dispersion of the short CFs in an epoxy matrix was achieved with a maximum number of surface charges. In addition, the AECNa-CF with good dispersion can be easily prepared, and comparing to the traditional modification methods, such as electrochemical treatment and plasma modification, the flexural strength and modulus of the treated CF/epoxy composites were greater than the corresponding values of the untreated CF/epoxy composites, almost without any weakening of the mechanical properties of CF.

Acknowledgment

This work was supported by the Specialized Research Fund for the Doctoral Program of Higher Education of China under Grant No. 20121201110002. The authors thank Tianjin Polytechnic University for Textile Auxiliary Co., Ltd. for the material support.

References

1. D.D.L. Chung, Cement Reinforced with Short Carbon Fibers: A Multifunctional Material, *Compos. B*, 2000, **31**(6), p 511–526
2. F. Rezaei, R. Yunus, and N.A. Ibrahim, Development of Short-Carbon-Fiber-Reinforced Polypropylene Composite for Car Bonnet, *Polym. Plast. Technol. Eng.*, 2008, **47**(4), p 351–357
3. O. Carneiro and J. Maia, Rheological Behavior of (Short) Carbon Fiber/Thermoplastic Composites. Part I: The Influence of Fiber Type, Processing Conditions and Level of Incorporation, *Polym. Compos.*, 2000, **21**(6), p 960–969
4. J. Wen, Z. Xia, and F. Choy, Damage Detection of Carbon Fiber Reinforced Polymer Composites Via Electrical Resistance Measurement, *Compos. B*, 2011, **42**(1), p 77–86
5. C. Wang, K.Z. Li, H.J. Li, G.S. Jiao, J. Lu, and D.S. Hou, Effect of Carbon Fiber Dispersion on the Mechanical Properties of Carbon Fiber-Reinforced Cement-Based Composites, *Mater. Sci. Eng. A*, 2008, **487**(1–2), p 52–57
6. J. Zhao, J. Hu, and Y. Liang, Study on Carbon Fiber Surface Characteristics and Its Dispersion in Water, *China Pulp Paper*, 2008, **27**(5), p 15–18 (in Chinese)
7. J.M. Park, Z.J. Wang, D.J. Kwon, G.Y. Gu, W.I. Lee, J.K. Park, and K.L. Devries, Optimum Dispersion Conditions and Interfacial Modification of Carbon Fiber and CNT-Phenolic Composites by Atmospheric Pressure Plasma Treatment, *Compos. B*, 2012, **43**(5), p 2272–2278
8. Y. Yang, Methods Study on Dispersion of Fibers in CFRC, *Cem. Concr. Res.*, 2002, **32**, p 747–750
9. M. Choi, B. Jeon, and I. Chung, The Effect of Coupling Agent on Electrical and Mechanical Properties of Carbon Fiber/Phenolic Resin Composites, *Polymer*, 2000, **41**(9), p 3243–3252
10. Z. Li, S. Wu, Z. Zhao, and L. Xu, Influence of Surface Properties on the Interfacial Adhesion in Carbon Fiber/Epoxy Composites, *Surf. Interface Anal.*, 2014, **46**(1), p 16–23
11. C. Van Oss and P. Costanzo, Adhesion of Anionic Surfactants to Polymer Surfaces and Low-Energy Materials, *J. Adhes. Sci. Technol.*, 1992, **6**(4), p 477–487
12. E. Manev and R. Pugh, Diffuse Layer Electrostatic Potential and Stability of Thin Aqueous Films Containing a Nonionic Surfactant, *Langmuir*, 1991, **7**(10), p 2253–2260
13. Y.K. Li, F.L. Zhao, and Y.F. Wang, Synthesis of Alkyl Phenol Polyoxyethylene Ether Carboxylate with Acetone as Solvent, *Acta Petrol. Sin. Pet. Process Sect.*, 2003, **19**(2), p 33–38
14. S.Y. Chen, Q.F. Hou, G.Q. Jian, Y.Y. Zhu, Y.S. Luo, Z. Wang, and W.J. Li, Synthesis and Performance Evaluation of Novel Alcohol Ether Carboxylate Surfactants for Alkali-Surfactant-Polymer Flooding, *Int. J. Oil Gas Coal Technol.*, 2014, **7**(1), p 52–67
15. C. Kaynak, O. Orgun, and T. Tincer, Matrix and Interface Modification of Short Carbon Fiber-Reinforced Epoxy, *Polym. Test.*, 2005, **24**(4), p 455–462
16. H.J. Zo, S.H. Joo, T. Kim, S.S. Pan, H.K. Jin, and J.S. Park, Enhanced Mechanical and Thermal Properties of Carbon Fiber Composites with Polyamide and Thermoplastic Polyurethane Blends, *Fiber Polym.*, 2014, **15**(5), p 1071–1077
17. J.M. Hofste and M. Kersten, Surface Charges in Blending Short Fibres with Polyethylene Powder, *J. Electrostat.*, 1998, **45**(1), p 69–78
18. Y.E. Krasik, A. Dunaevsky, and J. Felsteiner, Intense Electron Emission from Carbon Fiber Cathodes, *Eur. Phys. J. D*, 2001, **15**(3), p 345–348

19. S. Qin, M.P. Bradley, P.L. Kellerman, and K. Saadatmand, Measurements of Secondary Electron Emission and Plasma Density Enhancement for Plasma Exposed Surfaces Using an Optically Isolated Faraday Cup, *Rev. Sci. Instrum.*, 2002, **73**(3), p 1153–1156
20. Z.Q. Zhao and X.L. Chen, *The Technology Application of the Conductive and Antistatic Polymer Materials*, China Textile & Apparel Press, Beijing, 2006, p 165–210
21. C.Y. Huang, W.W. Mo, and M.L. Roan, Studies on the Influence of Double-Layer Electroless Metal Deposition on the Electromagnetic Interference Shielding Effectiveness of Carbon Fiber/ABS Composites, *Surf. Coat. Technol.*, 2004, **184**, p 163–169
22. H. Uchikawa, S. Hanehara, and D. Sawaki, The Role of Steric Repulsive Force in the Dispersion of Cement Particles in Fresh Paste Prepared with Organic Admixture, *Cem. Concr. Res.*, 1997, **27**, p 37–50
23. W. Kempiński, D. Markowski, M. Kempiński, and M. Śliwińska-Bartkowiak, Charge Carrier Transport Control in Activated Carbon Fibers, *Carbon*, 2013, **57**(6), p 533–536
24. N. Di Blasi, O. Di Briguglio, and V. Antonucci, Charge-Discharge Performance of Carbon Fiber–Based Electrodes in Single Cell and Short Stack for Vanadium Redox Flow Battery, *Appl. Energy*, 2014, **125**(2), p 114–122
25. Z. Xu, Y. Huang, C. Zhang, L. Liu, Y. Zhang, and L. Wang, Effect of γ-Ray Irradiation Grafting on the Carbon Fibers and Interfacial Adhesion of Epoxy Composites, *Compos. Sci. Technol.*, 2007, **67**, p 3261–3270
26. F. Vautard, P. Fioux, L. Vidal, J. Schultz, M. Nardin, and B. Defoort, Influence of the Carbon Fiber Surface Properties on Interfacial Adhesion in Carbon Fiber-Acrylate Composites Cured by Electron Beam, *Compos. A*, 2011, **42**(7), p 859–867
27. W. Song, A. Gu, G. Liang, and L. Yuan, Effect of the Surface Roughness on Interfacial Properties of Carbon Fibers Reinforced Epoxy Resin Composites, *Appl. Surf. Sci.*, 2011, **257**(9), p 4069–4074
28. N. Dumitrascu and C. Borcia, Determining the Contact Angle Between Liquids and Cylindrical Surfaces, *J. Colloid Interface Sci.*, 2006, **294**(2), p 418–422
29. Q. Peng, Y. Li, X. He, H. Lv, P. Hu, Y. Shang, C. Wang, R. Wang, T. Sritharan, and S. Du, Interfacial Enhancement Of Carbon Fiber Composites by Poly (Amido Amine) Functionalization, *Compos. Sci. Technol.*, 2013, **74**(4), p 37–42
30. Z. Dai, F. Shi, B. Zhang, M. Li, and Z. Zhang, Effect of Sizing on Carbon Fiber Surface Properties and Fibers/Epoxy Interfacial Adhesion, *Appl. Surf. Sci.*, 2011, **257**, p 6980–6985
31. H.H. Song, H.J. Oh, H.C. Lee, and S.S. Kim, The Effect of Post-Processing of Carbon Fibers on the Mechanical Properties of Epoxy-Based Composites, *Compos. B*, 2013, **45**(1), p 172–177
32. R. Zhang, Y. Huang, L. Liu, Y. Tang, D. Su, and L. Xu, Effect of Emulsifier Content of Sizing Agent on the Surface of Carbon Fibres and Interface of Its Composites, *Appl. Surf. Sci.*, 2011, **257**(8), p 3519–3523